materials

MDPI

Article

RC Medium-Rise Building Damage Sensitivity with SSI Effect

Liga Gaile *, Lasma Ratnika and Leonids Pakrastins

Faculty of Civil Engineering, Institute of Structural Engineering, Riga Technical University, LV-1048 Riga, Latvia; lasma.ratnika@rtu.lv (L.R.); leonids.pakrastins@rtu.lv (L.P.)

* Correspondence: liga.gaile_1@rtu.lv; Tel.: +371-2755-5757

Abstract: Global vibration-based methods in the field of structural health monitoring are intended to capture structural stiffness changes of buildings or other civil engineering structures. Natural frequencies of buildings or bridges are commonly used parameters to monitor these stiffness changes. Therefore, it is essential to clarify the limit at which this method is no longer sensitive enough to be useful for structural health monitoring purposes. This paper numerically investigates the effect of structural damage and soil–structure interaction on cellular-type reinforced concrete buildings' natural frequencies. These buildings are a common housing stock of Eastern Europe but are rarely investigated in this context. Comparisons with a reinforced concrete frame and infill structure building are made. Finite element models representing three structural system types of nine-story reinforced concrete buildings were used for the numerical simulations. Furthermore, a five-story finite element model was used for a damage sensitivity comparison. It is established that, for cellular-type structure buildings to detect damage comparable to that investigated in the paper, structural health (fixed base model frequency) should be monitored directly. Then, a statistical significance level for frequency changes of no more than 0.1% should be adopted. Conversely, the rocking frequency is a very sensitive parameter to monitor building base condition changes. These changes are often a cause of the cracking of building elements.

Keywords: structural health monitoring; soil–structure interaction; reinforced concrete buildings; natural frequencies; rocking frequencies; damage detection

Citation: Gaile, L.; Ratnika, L.; Pakrastins, L. RC Medium-Rise Building Damage Sensitivity with SSI Effect. *Materials* **2022**, *15*, 1653. https://doi.org/10.3390/ma15051653

Academic Editor: Gintaris Kaklauskas

Received: 29 December 2021
Accepted: 21 February 2022
Published: 23 February 2022

1. Introduction

The future development of smart buildings is unthinkable without introducing instrumented building monitoring systems that continuously monitor the structural performance of a building and provide early warning to building managers of signs of structural damage risks of degradation. Structural health monitoring is a scientific and engineering discipline that develops these types of solutions. Vibration-based methods for monitoring changes in the global stiffness of structures play an essential role in this field. This method is generally used for monitoring the technical condition of major high-rise buildings or bridges [1] with the development of suitable sensitive and accurate sensor systems [2]; it is also becoming possible to monitor low- and medium-rise structures, despite very low vibration amplitudes, which are on the order of 10^{-6} m/s^2–10^{-4} m/s^2 [3] and caused by ambient ground vibration.

Natural frequencies are the most commonly used parameters to identify building stiffness change using vibration-based methods [4]. The reason is the currently well-developed operational modal analysis (OMA) algorithms for the identification of these parameters from ambient vibrations [5] and developed methods for modeling environmental and operational variation effects (EOVs) on frequencies [6].

Therefore, a practical question becomes important: What kind of structural damage, and to what extent, is reflected in changes of natural frequencies of buildings? Most studies deal with analyzing individual elements in this context [7]. Some of the experimental

studies on the impact of structural damage on whole-structure natural frequencies can be found in [8,9].

From these investigations, one of the crucial aspects to consider in medium-rise buildings is the soil–structure interaction effect (SSI), particularly the inertial SSI effect [10]. The effect is most pronounced when the building is located on weak or moderately weak soils [11]. In this case, the natural frequencies of the building are significantly reduced compared to a fixed base model. This poses a problem in identifying stiffness changes from changes in a modal parameter of the structure such as frequency since its change due to structural damage has a decreasing effect on the fundamental and other natural frequencies when the SSI effect is stronger [12].

One way to overcome this problem could be by performing a modal decomposition so that the shapes associated with the structural vibrations of the building are separated from the shape associated with the rocking motion. Then, the structural damage can be analyzed using the fixed foundation model, and the changes in the soil parameters (e.g., due to groundwater fluctuations [13]) can be analyzed using the rocking mode shape frequency.

In this case, it is appropriate to model the building as a multi-mass model [14] (see Figure 1), so that low-amplitude ambient vibrations can be approximated as elastic deformations [15].

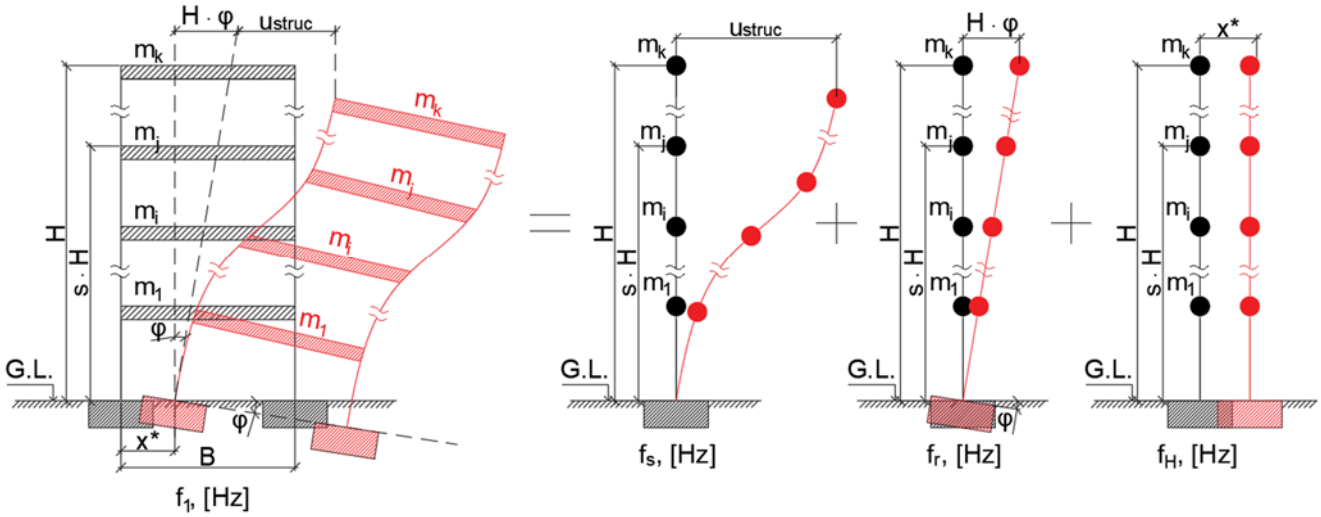

Figure 1. Multi-mass model scheme of building frame; f_1—fundamental frequency, f_s—frequency of shear frame action, f_r—frequency of rocking action, f_h—frequency of horizontal movement (not considered in this paper further), u_{struc}—shear deformation of frame, H—building height, x*—horizontal displacement.

Depending on the geometry of the building, the shape of the lateral mode is as for a Euler–Bernoulli beam, pure shear beam, or somewhat in between. Hans and Boutin [16] developed a generic beam governed by a differential equation of the sixth degree to comprehend different types of buildings (see Equation (1)). The elastic parameters used in the equation are derived from elastic properties of the generic story under static shear or bending deformations. Depending on the structural behavior, the general model can degrade into a simpler model.

$$((E{\cdot}I_\mu{\cdot}E{\cdot}I)/K){\cdot}U^{(6)} - (E{\cdot}I_\mu + E{\cdot}I){\cdot}U^{(4)} - ((E{\cdot}I)/K){\cdot}\Lambda{\cdot}\omega^2{\cdot}U^{(2)} + \Lambda{\cdot}\omega^2{\cdot}U = 0, \quad (1)$$

where $U^{(x)}$ is the horizontal displacement of the floors of the structure, K is the shear stiffness, EI is the global bending stiffness, EI_μ is the inner bending stiffness, Λ is the lineic density of structural material, and ω is the circular frequency.

However, there is no deformation of the structure itself in the rocking mode, but only a rotation of the foundation about a pivot point. The modal decomposition method

was described in [17] where the coupling of all vibration modes with rocking action was considered.

This paper aims to numerically investigate the effect of structural damages on the natural-frequency changes of reinforced concrete buildings. Therefore, it contributes to understanding which kinds of medium-rise structures are appropriate for using the global vibration-based methods based on frequency sensitivity to the structural damage. In addition, curves are developed to estimate the percentage of frequency change using a fixed foundation model that is reflected in the percentage frequency change when the SSI effect through the rocking frequency is considered. This type of information can help at the planning stage, when the number and location of sensors and identification techniques need to be selected for structural monitoring, helping to understand whether the rocking motion of the building also needs to be identified separately. Particular attention is paid to cellular-type structures that are rarely investigated in this context. The term cellular means that the building structure is similar to stacked boxes, where each box can be considered as a cell, but the elements of the cells are structural elements.

It is established that, for cellular-type structure (nine-story) buildings, to detect damage comparable to that investigated in the paper, structural (fixed base model) frequency should be monitored directly. The statistical significance level for frequency changes should be adopted at no more than 0.1%.

Conversely, the rocking frequency is a very sensitive parameter to monitor building base condition changes that are often a cause of cracking of building elements and could be very useful.

2. Materials and Methods

2.1. Rocking and Structural Frequencies of Medium-Rise Reinforced Concrete Buildings

Full-scale experiments show that response due to ambient ground vibrations can be considered elastic for medium-rise buildings [18]. This means that the superposition principle applies, and the vibration modes of the structure can be decomposed as shown in Figure 1. Then, the fundamental frequency in the direction considered can be approximated by the following well-known relationship:

$$1/f_1{}^2 = 1/f_s{}^2 + 1/f_r{}^2, \quad (2)$$

where f_1 is the fundamental frequency in the direction considered, f_s is the structural fixed base model frequency in the direction considered, and f_r is the rocking frequency in the direction considered.

Typical fundamental frequencies are known from a number of experimental studies [19–21] and are given in Table 1.

Table 1. Fundamental frequency ranges of buildings [22].

Number of Stories (Number of Assessed Buildings)	Typical Fundamental Frequency Range, Hz	Mean (Standard Deviation), Hz
1–3 (63)	1.2–12.5	6.1 (2.8)
4–5 (108)	0.7–6.5	3.8 (1.2)
6–7 (91)	0.8–4.8	2.8 (0.8)
8–9 (71)	0.7–3.3	2.1 (0.6)
10–12 (86)	0.7–3.5	1.9 (0.6)
13–16 (53)	0.4–2.2	1.3 (0.4)

The experimental frequencies shown in Table 1 include the frequency reduction due to the SSI effect. Therefore, by using the values in Table 1 as input parameter f_1 in Equation (2), it is possible to determine theoretically which pairs of fundamental modal components—structural frequency f_s and rocking frequency f_r—are even possible for a given range of buildings.

$$f_{min} \leq (f_s{}^2 \cdot f_r{}^2/(f_s{}^2 + f_r{}^2))^{1/2} \leq f_{max}, \text{ where } f_r \leq f_s. \quad (3)$$

Research has shown [23] that the rocking frequency f_r is generally lower than structural frequency f_s. If, due to the high stiffness of the structure, it acts more and more like a rigid body on the ground, then the rocking frequency effect increases [24]. Therefore, an additional constraint is introduced into Equation (3) whereby rocking frequency is less than or equal to the structural frequency. The system of inequalities is solved numerically by the simulation to obtain the possible combinations of modal components when f_s is taken in the range of 0.4–15 Hz.

Depending on the accuracy of the modal parameter identification, different statistical significance levels can be adopted for frequency changes due to structural damage, e.g., 0.1% (0.001), 0.5% (0.005), 1% (0.01), and 5% (0.05). It is, therefore, logical to consider structural frequency variations Δf_s due to damage at least in the range 0–5%. This variation can be expressed as a percentage difference between the reference-state structural frequency f_s and the structural frequency of damaged structure d_s.

$$\Delta f_s = 100\% \cdot (f_s - d_s)/f_s, \tag{4}$$

where Δf_s denotes structural frequency changes due to structural damage (%), f_s is the initial structural frequency (reference state), and d_s is the fundamental structural frequency of the damaged structure (modeled with fixed foundation).

The frequency change including the effects of SSI can be expressed as a percentage difference between the reference-state fundamental frequency f_1 and the fundamental frequency of damaged structure d.

$$\Delta f_1 = 100\% \cdot (f_1 - d)/f_1. \tag{5}$$

In Equation (5), to find $(f_1 - d)$, a modification of Equation (2) can be used. Then, estimation of the frequency change $(f_s - d_s)$ using a fixed foundation model that is reflected in the frequency change $(f_1 - d)$ when the SSI effect through the rocking frequency is considered can be achieved using Equation (6).

$$(f_1 - d) = ((f_s - d_s)^2 \cdot f_r{}^2/((f_s - d_s)^2 + f_r{}^2))^{1/2}. \tag{6}$$

2.2. Data for the Numerical Study

In order to investigate the effect of the rocking frequency and structural changes on the natural frequency of three different building types, the following nine-story reference numerical models were created in the finite element model (FEM) software Dlubal RFEM using beam and plate finite elements (see Figure 2):

- cellular structure, reinforced concrete (RC) building (reference model #1);
- frame structure, RC building (reference model #2);
- frame structure with masonry infill walls, RC building (reference model #3).

The outer geometry was the same for all the models. The height of the buildings was 26.11 m, with plan dimensions of 11.620 × 33.84 m. The geometric dimensions of the individual elements are summarized in Table 2. Material constants for all reference models were taken as the same: modulus of elasticity 2490 kN/cm^2, shear modulus 1037.50 kN/cm^2, Poisson's ratio 0.2, and specific weight 25 kN/m^3. For infill walls, material constants were as follows: modulus of elasticity 1800 kN/cm^2, shear modulus 750 kN/cm^2, Poisson's ratio 0.2, and specific weight 17.50 kN/m^3.

Masonry infill was included in the appropriate manner in the finite element model according to [25]. Connections of the plate elements of the cellular precast building were modeled as a hinge joint between two surfaces. A fixed base model was considered for all reference buildings because the frequency sensitivity to damage considering the SSI effect could be later modified by the relationship obtained in this paper (see Section 3). The building structure itself was modeled elastically due to the fact that, under ambient vibrations, it has been experimentally proven that it behaves in this manner [18]. Natural

frequencies of models were calculated using the Lanczos iterative method suitable for large models [26].

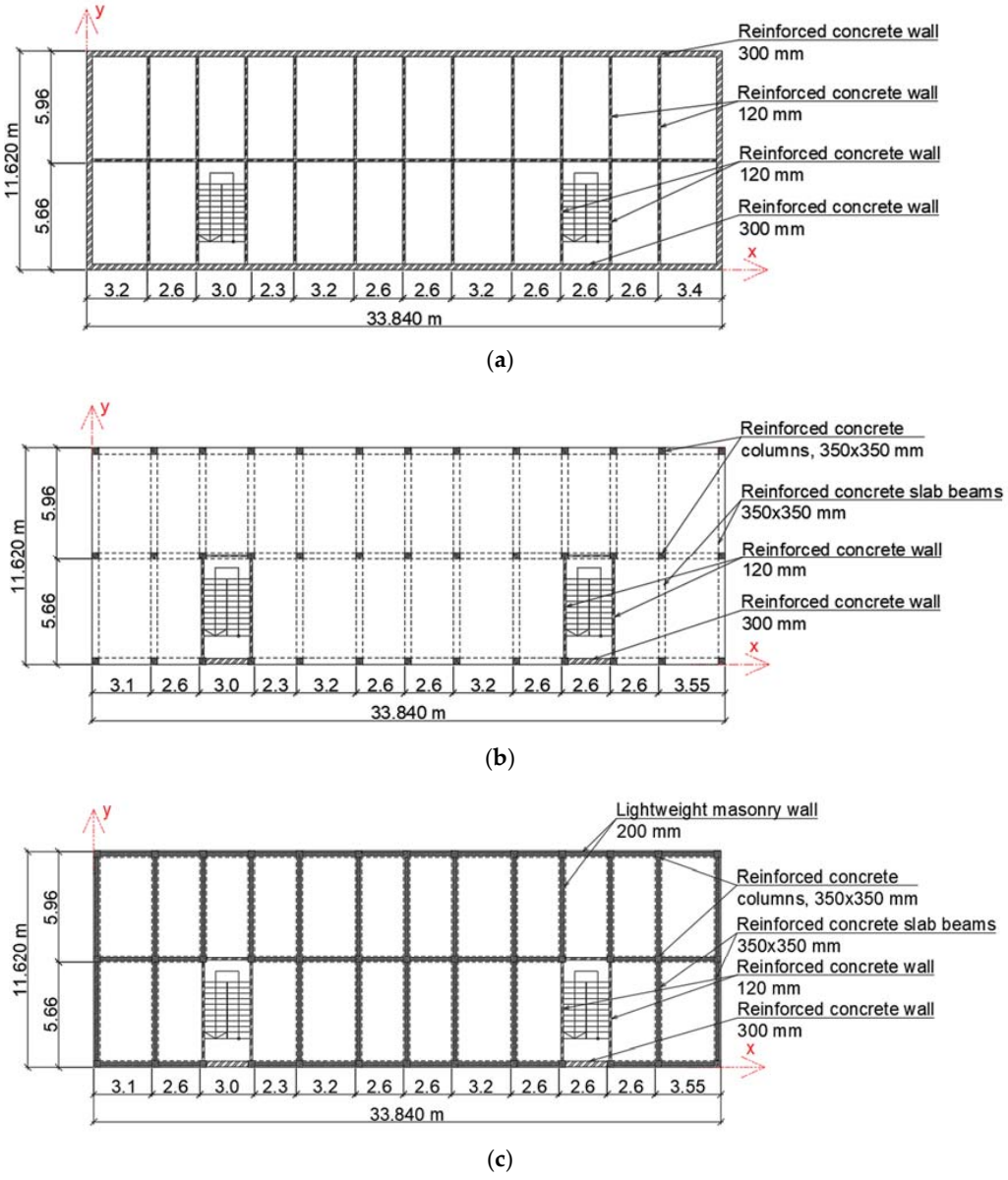

Figure 2. Principal schemes of investigated FEM reference models: (**a**) cellular structure, RC building (reference model #1); (**b**) frame structure, RC building (reference model #2); (**c**) frame structure with masonry infill walls, RC building (reference model #3).

The structural damage to the building was assumed to be localized wall damage reflecting, for example, a newly formed doorway that was not foreseen in the original project and sometimes could be built illegally without the approval of the relevant authorities. Each model type had 11 interior wall planes in the longitudinal direction (y-direction). Structural damage was assumed for each interior wall plane until the symmetry axis of the building was reached. It is expressed as a percentage that was calculated as the ratio of the total wall plane area to the removed or damaged part of the wall area. For each plane, a damage percentage of 13% was assumed, and changes in the natural frequencies of the building were recorded (see also Section 3.2).

Table 2. Structural geometry description of the numerical reference models.

Type of Element	Model #1	Model #2	Model #3
Main vertical elements	Shear walls with thickness 120 mm	Columns 350 × 350	Columns 350 × 350
Floor slabs	100 mm	100 mm	100 mm
Roof slab	100 mm	100 mm	100 mm
Infill walls	-	-	Lightweight masonry wall 200 mm
Foundation	Strip foundation 800 × 400 (h) mm	Strip foundation 800 × 400 (h) mm	Strip foundation 800 × 400 (h) mm
Global stiffness (direction *x*)	1,617,143 kN/m	27,610 kN/m	1,415,000 kN/m
Global stiffness (direction *y*)	1,197,857 kN/m	27,180 kN/m	1,081,935 kN/m
Total mass of building [1]	8,386,020.66 kg	3,741,773.96 kg	8,308,993.32 kg

[1] The combination of load used to calculate the natural frequencies was C = 1.0 × live load + 1.0 × self-weight of construction and layers.

The global structural stiffness of the building described in Table 2 was calculated using FEM as the reference force applied to the building wall plane in *x*- or *y*-directions divided by the displacement of the building in *x*- or *y*-directions, respectively.

Using the three types of reference models and Equation (2), and supplementing these models with shallow foundations on three typical soils (the composition of which is summarized in Tables 3–5), the theoretical rocking frequency was also derived. Soil under the foundations was idealized as a homogeneous half-space with a linear–elastic, isotropic material [27]. The stiffness and damping properties of the soil were modeled using vertical and horizontal springs calculated for each soil type. The foundation parameters were calculated iteratively by means of a nonlinear method for every finite element depending on the loading from the building.

Table 3. Soil materials of soil type I.

Soil Description	Soil Layer Parameters					
	Specific Weight		Modulus of Elasticity, MN/m^2	Poisson's Ratio ν	Thickness, m	Ordinate from Ground Level, m
	Unsaturated Weight γ, kN/m^3	Saturated Weight γ_{sat}, kN/m^3				
Sand, closely graded	17.0	19.0	30.0	0.30	0.80	0.80
Sand	19.0	21.0	30.0	0.30	3.0	3.80
Dusty sand	18.0	20.3	18.0	0.30	4.0	7.80
Sand, gravelly sand	18.0	20.0	20.0	0.30	8.20	16.0

Table 4. Soil materials of soil type II.

Soil Description	Soil Layer Parameters					
	Specific Weight		Modulus of Elasticity, MN/m^2	Poisson's Ratio ν	Thickness, m	Ordinate from Ground Level, m
	Unsaturated Weight γ, kN/m^3	Saturated Weight γ_{sat}, kN/m^3				
Sand, closely graded	17.0	19.0	30.0	0.30	0.80	0.80
Sand	19.0	21.0	30.0	0.30	3.0	3.80
Clay, low plasticity	19.0	19.5	2.50	0.42	4.50	8.30
Sand–clay mixture	18.0	19.0	10.0	0.35	7.70	16.0

Table 5. Soil materials of soil type III.

Soil Description	Soil Layer Parameters					
	Specific Weight		Modulus of Elasticity, MN/m^2	Poisson's Ratio ν	Thickness, m	Ordinate from Ground Level, m
	Unsaturated Weight γ, kN/m^3	Saturated Weight γ_{sat}, kN/m^3				
Sand, closely graded	17.0	19.0	30.0	0.30	0.80	0.80
Sand	19.0	21.0	30.0	0.30	3.0	3.80
Peat	10.40	10.40	1.0	0.40	0.80	4.60

Table 5. *Cont.*

Soil Description	Soil Layer Parameters					
	Specific Weight		Modulus of Elasticity, MN/m^2	Poisson's Ratio ν	Thickness, m	Ordinate from Ground Level, m
	Unsaturated Weight γ, kN/m^3	Saturated Weight γ_{sat}, kN/m^3				
Dusty sand	18.0	20.3	18.0	0.30	3.7	8.30
Sand, gravelly sand	18.0	20.0	20.0	0.30	7.7	16.0

For investigations of the SSI effect on the building frequencies, nine FEM models were considered, whereas, for the damage sensitivity simulations, 192 FEM models were calculated.

3. Results

3.1. Modal Components of Medium-Rise RC Buildings

Theoretically possible ranges for the modal components structural frequency fs and rocking frequency f_r of the first vibration mode for rigid buildings when fr < fs are summarized in Figure 3. These ranges were defined according to the methodology described in the previous section. These obtained ranges could be useful to assess experimental result credibility when performing modal parameter identification in practice.

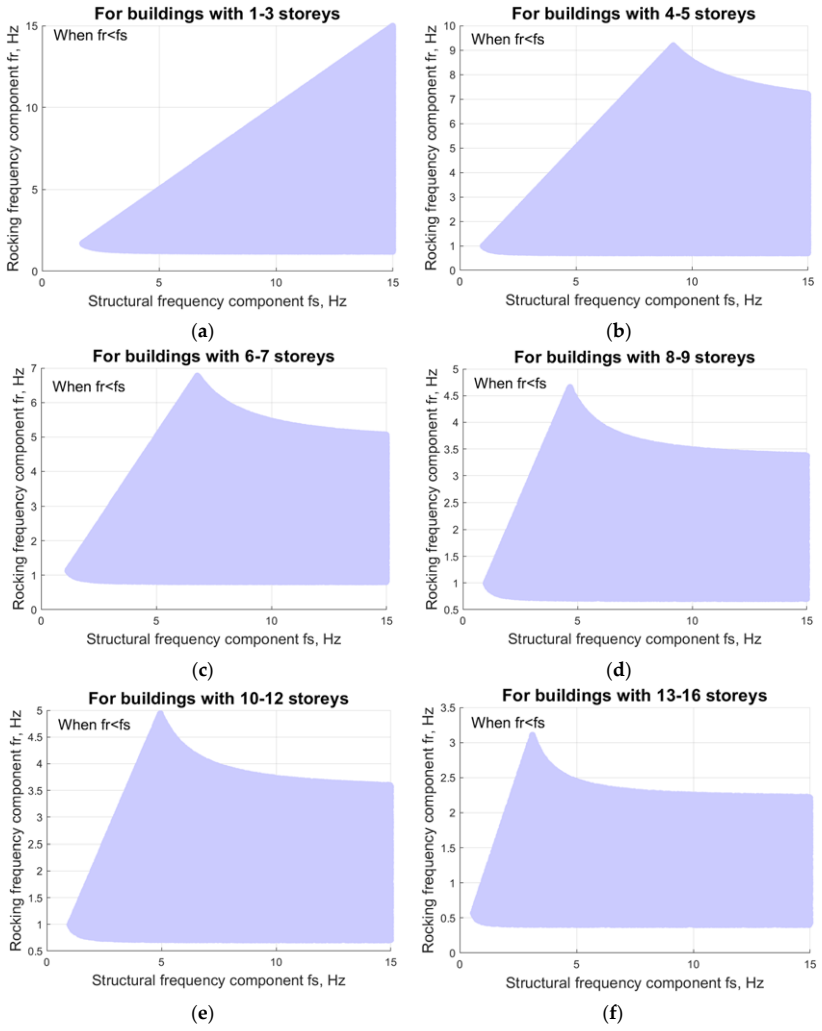

Figure 3. Modal component ranges of the first vibration mode for buildings: (**a**) 1–3 stories; (**b**) 4–5 stories; (**c**) 6–7 stories; (**d**) 8–9 stories; (**e**) 10–12 stories; (**f**) 13–16 stories.

Table 6 summarizes the results obtained from the finite element calculations, decomposing separately the contribution of each modal component using Equation (2) for the three vibration modes (Figure 4) and showing the ratio between structural mode and the mode with SSI effects including f_s/f_1.

Table 6. Structural frequencies and their modal components for building reference models.

Type of Soil	Para-Meter [2]	Mode # of Model #1			Mode # of Model #2			Mode # of Model #3		
		Lateral	Longitudinal	Torsional	Lateral	Longitudinal	Torsional	Lateral	Longitudinal	Torsional
I	f_1	1.255	1.973	2.171	0.518	0.630	0.702	1.215	1.897	2.128
	f_s	5.339	6.800	7.481	0.854	0.903	1.077	4.965	5.844	6.392
	f_r	1.291	2.062	2.269	0.652	0.879	0.926	1.253	2.006	2.257
	f_s/f_1	4.25	3.45	3.45	1.65	1.43 [3]	1.53	4.09	3.08	3.00
II	f_1	0.867	1.628	2.164	0.433	0.603	0.670	0.838	1.573	2.113
	f_s	5.339	6.800	7.481	0.854	0.903	1.077	4.965	5.844	6.392
	f_r	0.879	1.677	2.261	0.518	0.810	0.856	0.850	1.633	2.239
	f_s/f_1	6.16	4.18	3.46	1.97	1.50	1.61	5.92	3.72	3.03
III	f_1	1.025	1.796	2.166	0.476	0.615	0.684	0.993	1.73	2.118
	f_s	5.339	6.800	7.481	0.854	0.903	1.077	4.965	5.844	6.392
	f_r	1.044	1.862	2.263	0.573	0.840	0.886	1.013	1.811	2.245
	f_s/f_1	5.21	3.79	3.45	1.79	1.47	1.57	5.00	3.38	3.02

[2] Parameter f_s does not depend on soil type; [3] the lowest ratio value obtained.

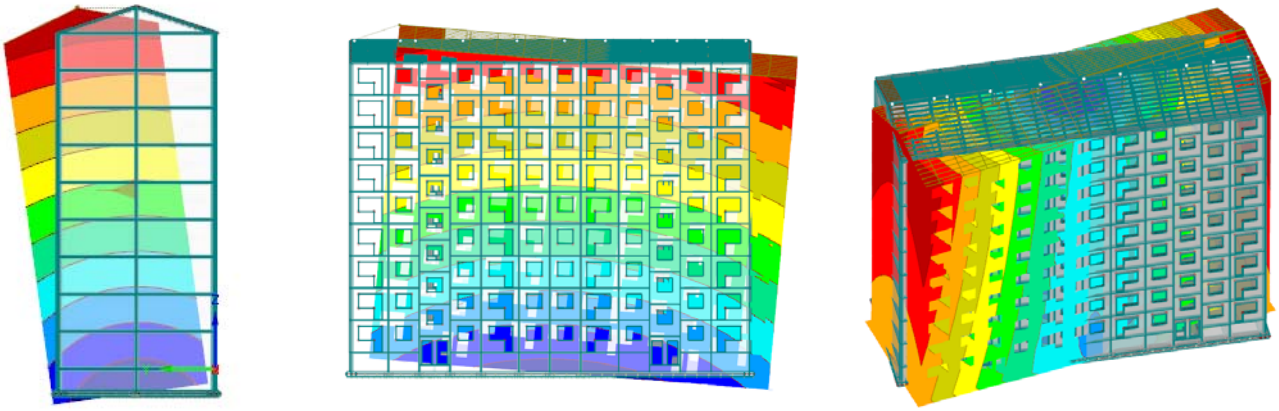

(**a**) (**b**) (**c**)

Figure 4. Fundamental vibration modes in each direction: (**a**) lateral mode; (**b**) longitudinal mode; (**c**) torsional mode.

This f_s/f_1 relationship reveals that the rocking frequency plays a very important role in the value of the lowest natural frequency, and its importance increases with the rigidity of the building on weaker soils. In none of the cases considered was $f_r > f_s$ found; hence, the lowest ratio value obtained was 1.43. This is as it should be since the lowest possible value of the f_s/f_1 ratio is $\sqrt{2}$, which follows from Equation (2) in the case of $f_s = f_r$.

A lower value denotes greater sensitivity of the fundamental frequency to the building damage scenario. For all soil types, the highest ratio f_s/f_1 values were found for the vibration modes in the direction of the smaller width of the building, which means that, if changes in soil parameters are to be monitored, it is valuable to look at the natural frequency of this vibration mode; however, if the structure itself is to be monitored, the torsional mode and lateral vibrational mode in the stiffer direction of the building should be looked at.

Table 7 analyzes the variation of rocking frequencies with soil type for buildings on shallow foundations.

Table 7. Rocking frequency f_r according to soil type.

Type of Soil	Parameter [1]	Mode # of Model #1			Mode # of Model #2			Mode # of Model #3		
		Lateral	Longitudinal	Torsional	Lateral	Longitudinal	Torsional	Lateral	Longitudinal	Torsional
I	f_r	1.291	2.062	2.269	0.652	0.879	0.926	1.253	2.006	2.257
	Δf_r	-	-	-	-	-	-	-	-	-
II	f_r	0.879	1.677	2.261	0.518	0.810	0.856	0.850	1.633	2.239
	Δf_r	46.87%	22.96%	0.35%	25.87%	8.52%	8.18%	47.4%	22.84%	0.80%
III	f_r	1.044	1.862	2.263	0.573	0.840	0.886	1.013	1.811	2.245
	Δf_r	23.66%	10.74%	0.27%	13.79%	4.64%	4.52%	23.69%	10.76%	0.55%

[1] Where Δf_r is the percentage change in rocking frequency with respect to the building on type I soil for a given model and mode.

It is clear that the soil type influences the rocking frequencies for all building types, especially for the first vibration mode in the narrowest building direction. For rigid buildings such as reference models #1 and #3, changes in soil composition have little effect on the rocking components of the torsional vibration mode.

According to the results in Table 7, the rocking frequency is a sensitive parameter for medium-height buildings to monitor changes in the building base condition. Changes in this parameter could promptly highlight future problems such as damage to the building structure due to uneven settlement, leading to cracking or undesirable displacements of horizontal members.

3.2. Effect of Structural Changes on the Natural Frequencies of RC Building

Structural alternations of buildings change the structural frequency f_s (fixed foundation model). However, because rocking frequency considerably lowers the fundamental frequency of a building, these changes can have a minor effect on the fundamental frequency itself. To evaluate this effect, 10,000 simulations were performed with randomly selected values of rocking frequency f_r and structural frequency f_s, as well as different levels of structural frequency changes δf_s. Fundamental frequency f_1 and change in fundamental frequency δf_1 were calculated according to the methodology in Section 2.1, and the results are presented in Figure 5.

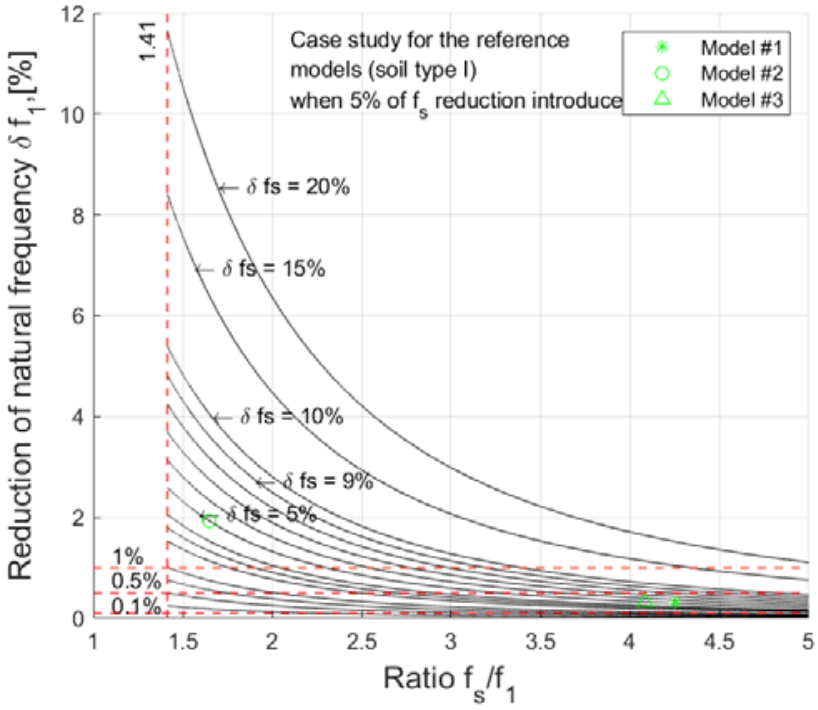

Figure 5. Sensitivity of natural frequency reduction to structural frequency f_s reduction.

When analyzing the percentage change of the first vibration mode as a function of the building frequency ratio f_s/f_1 (under the condition that $f_r \leq f_s$), the curves tended asymptotically to a value of $\sqrt{2}$, with at most half of the structural frequency change being reflected in the first vibration mode (see Figure 5). If this ratio increases (i.e., the structure becomes stiffer relative to the deformability of the foundation), then the possibility of detecting structural damage from the frequency change of the first vibration mode decreases rapidly as the curve follows the power relationship. In Figure 5, the curves from lower to higher are plotted for the following f_s variations: 0.5%, 1%, 1.5%, 2%, 3%, 3.5%, 4%, 5%, 6%, 7%, 8%: 9%, 10%, 15%, and 20%.

Comparing the values in Table 7 with the graph in Figure 5, it follows that, for cellular or RC frame buildings with infill, where the change in the first frequency in each direction or in torsional frequency when structural damage changes the structural frequency f_s by less than 10%, the change in f_1 is below the significance threshold of 0.5%. In this case, the solution is to identify and directly monitor the modal component f_s.

To understand how much damage to the building is required to produce sufficient changes in f_s for successful identification by operational modal analysis techniques, the most robust Model #1 was analyzed, successively taking out three panels at a time at each location (see Figure 6). In this case, a damage of 13% was calculated according to the methodology described in the previous section.

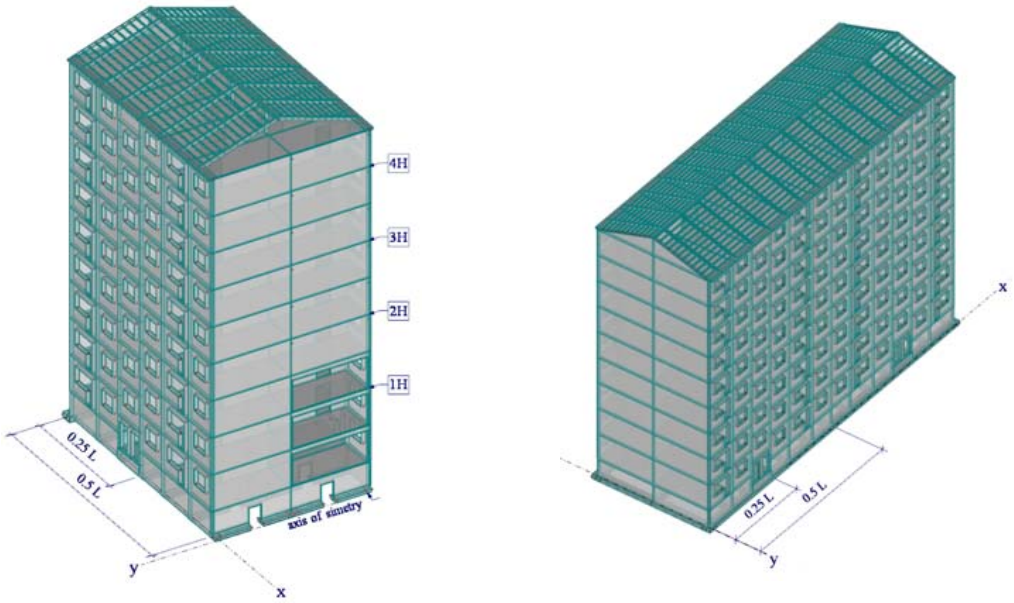

(**a**) (**b**)

Figure 6. Damage locations for the reference model #1: (**a**) building section; (**b**) FE model of the building.

The variation of structural frequency f_s due to the damage scenario for reference Model #1 depending on the damage location in the building plan or height is displayed in Figures 7 and 8. The horizontal axis shows the dimension of the building in plan n × L, where 0.5 L corresponds to the axis of symmetry of the building in plan. The vertical axis corresponds to the building height s × H, which is up to the middle panel removed. (see Figure 6). To compare results of buildings with a different number of stories, a five-story building model was also chosen (with the same damage level of 13%).

As expected, the first vibration mode was the most sensitive for global damage identification purposes. The plot in Figure 8a (at distance 0.23 L) reveals that damage in walls around stiffness cores, e.g., staircases for lower buildings, influences a more fundamental frequency change of the building itself. Damage located in the middle of the building can be identified more easily when using the first lateral mode on the lower floors, while damage at the ends of the building can be identified more easily when using the torsional

mode on the lower floors. This means that, for damage detection in building vertical elements that are located up to the midweight of the building, a statistical significance level of 0.25% (for frequency identification) can be adopted. However, the main conclusion is that statistical significance levels for frequency changes should be adopted at no more than 0.1% for such rigid buildings when aiming for damage detection in all vertical loadbearing building elements. When damage is even smaller than the damage considered in this study, monitoring of the structure itself using global vibration-based methods is not applicable for damage identification in this case.

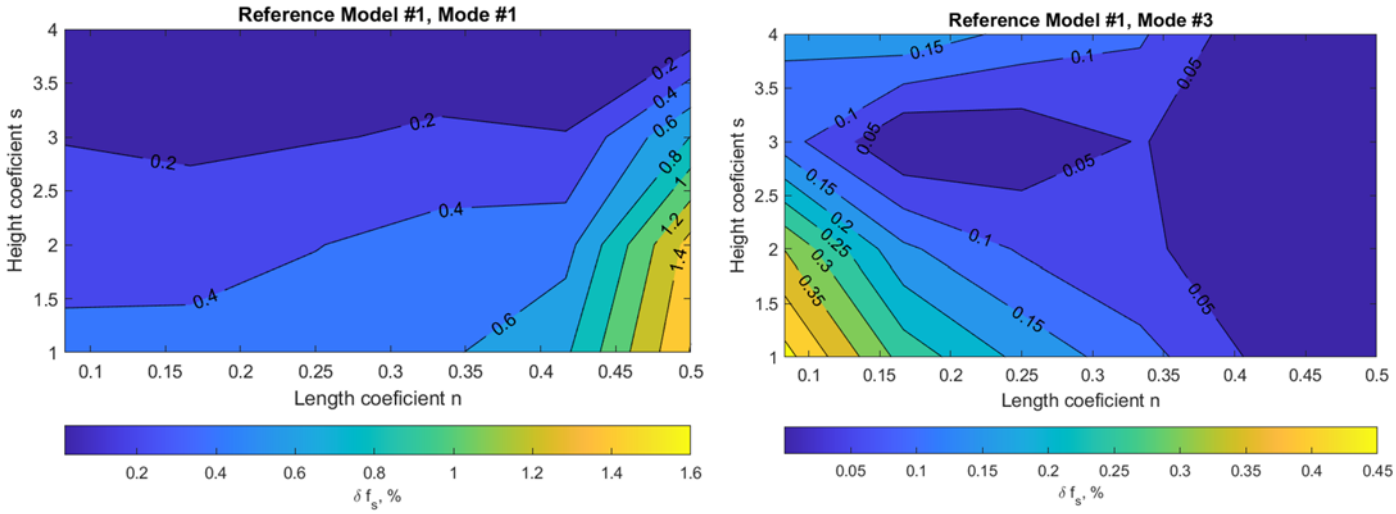

(**a**) (**b**)

Figure 7. Variation of structural frequency f_s due to damage scenario for reference nine-story model #1: (**a**) mode #1 (lateral); (**b**) mode #3 (torsional).

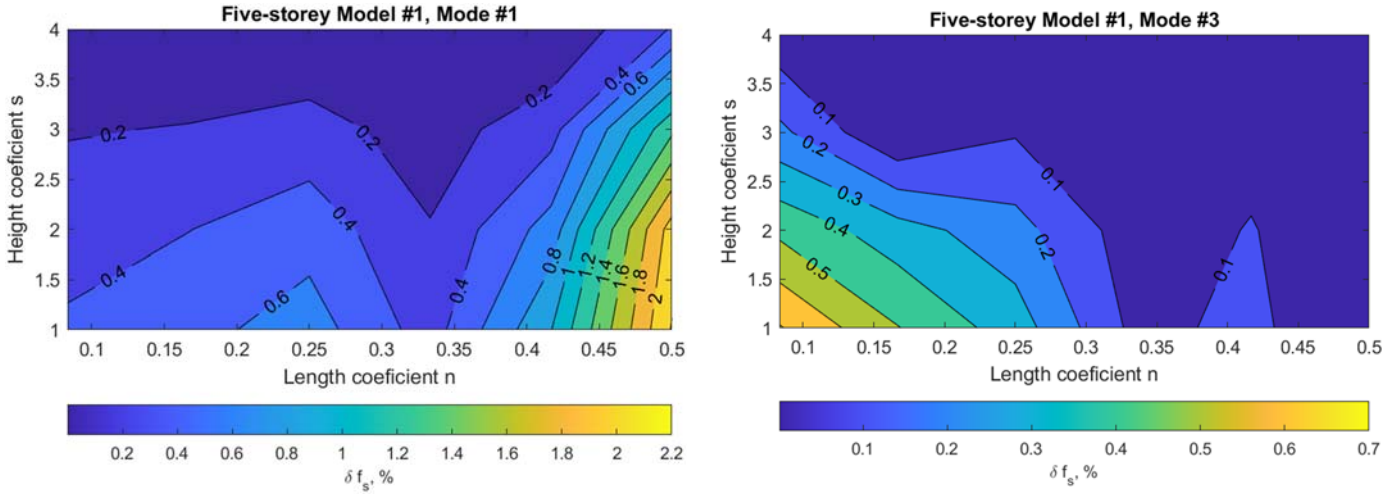

(**a**) (**b**)

Figure 8. Variation of structural frequency f_s due to damage scenario for reference five-story Model #1: (**a**) mode #1 (lateral); (**b**) mode #3 (torsional).

4. Discussion

The prototype for numerical models was a building widely used as a residential building in the former USSR (Figure 9a). The initiation of instrumented monitoring for such buildings is particularly relevant as they are approaching the end of their design life. Extending the lifetime of this type of housing stock would be a significant economic and ecological investment.

(**a**) (**b**)

Figure 9. Cracks in residential buildings: (**a**) cracks in building façade panels; (**b**) cracks in building loadbearing walls.

Frequently, damage or cracks in such buildings are caused by changes in ground conditions due to washouts, groundwater fluctuations, or nearby construction works, which are often difficult to prove for building owners. Therefore, a continuous monitoring system that identifies structural or base condition changes early could contribute to better management of those buildings. Examples of such cracks are shown in Figure 9b.

The results of the study presented in the previous section highlight the need for modal component detection by an operational modal analysis. These components are the structural frequency f_s corresponding to the fixed base condition and the rocking frequency f_r corresponding to the swaying motion of the building as a rigid body. There have been some attempts to do this on real buildings under ambient vibrations, e.g., [28,29]. However, the rocking motion for buildings has been mostly studied in the field of earthquake engineering as a technique to reduce and predict a seismic response [30].

In [31], the authors presented a linear finite element model (FEM) for damage identification of a 10-story reinforced concrete building using ambient vibration measurements. Damage was induced in the real building by experimentally removing six exterior infill walls. In that study, as in this one, it was found that the frequency reduction for mode #3 (torsional mode) was significantly smaller compared to that for modes #1 and #2. The reduction in the identified natural frequencies between the initial and the damage state for mode #1 and mode #2 was 6.25% and 7.19%; however, the reduction for mode #3 was only 0.6%. Compared to this study, when the maximum theoretical fundamental frequency change was only 1.4%, the experimental building had lower global stiffness and higher damage extent (six removed panels).

The parameter f_s/f_1 showing the ratio between structural mode frequency and structural frequency with SSI effects included denotes the building frequency sensitivity to structural damage events. This parameter obtained for a frame structure building is comparable to that found in similar studies (e.g., [12]). It is roughly 1.5 for soft soils. However, for cellular-type structures, it is more than 3, which is rarely found in the literature.

As for medium-height buildings such as cellular or frame buildings with masonry infills, the most sensitive modal component was found to be the rocking frequency f_r. Thus, if modal updating is intended, the correct updating of the boundary conditions of the supports should receive the most attention. Rocking frequency is a parameter that is worthy of further study because of its sensitivity to change and because there is very little experimental research in this context. For example, it can be used to identify the causes of building damage such as cracking, as well as to develop an early warning system for building managers.

5. Conclusions

This study investigated the components of natural frequencies for medium-rise buildings, namely, rocking frequency and structural frequency. Charts of theoretically possible rocking and structural frequency pairs were presented for buildings with a different number of stories. These charts can be used for full-scale experimental investigation validation in practice, thus allowing a quick assessment of whether an experimentally identified structural or rocking frequency is realistic for the relevant type of building.

Simulations on three types of FEM models for nine-story buildings (cellular structure, moment-frame structure, and moment-frame structure with infills) revealed the sensitivity of rocking frequency to the changes in the foundation of medium-rise buildings. This especially holds for the cellular-type structural buildings or buildings with masonry infills. Therefore, it is suggested to consider rocking frequency as a damage-sensitive parameter in structural health monitoring applications for medium-rise buildings.

The effect of minor structural changes and their location (represented as widened door openings in three places of nine-story and five-story cellular-type buildings) was investigated by performing simulations on 192 FEM models. The main conclusions are as follows:

- For structural damage monitoring purposes of stiff medium-rise buildings (cellular type or moment-frame with infills), structural frequency (fixed base model) should be used instead of fundamental frequency (which includes the SSI effect); practically, this can be done by firstly identifying rocking frequency and fundamental frequency before calculating structural frequency;
- Statistical significance levels for structural frequency changes should be adopted at no more than 0.1% for such rigid buildings when aiming for damage detection in vertical loadbearing building elements. This requires experimental modal identification procedures performed with less than 0.1% uncertainty.

Further introduction of real damage for full-scale buildings and performing ambient vibration measurements on the updated reference models and damaged buildings are of interest to quantitatively compare the obtained results in this study.

Author Contributions: Conceptualization, L.G.; methodology, L.G.; formal analysis, L.G., L.R. and L.P.; investigation, L.G., L.R. and L.P.; data curation, L.R.; writing, L.G. and L.R.; visualization, L.R.; supervision, L.G. All authors have read and agreed to the published version of the manuscript.

Funding: This work was supported by the European Regional Development Fund within the Activity 1.1.1.2 "Postdoctoral Research Aid" of the Specific Aid Objective 1.1.1 "To increase the research and innovative capacity of scientific institutions of Latvia and the ability to attract external financing, investing in human resources and infrastructure" of the Operational Program "Growth and Employment" (No.1.1.1.2/VIAA/3/19/393).

Institutional Review Board Statement: Not applicable.

Informed Consent Statement: Not applicable.

Data Availability Statement: Data are available on request to the authors.

Conflicts of Interest: The authors declare no conflict of interest.

References

1. Avci, O.; Abdeljaber, O.; Kiranyaz, S.; Hussein, M.; Gabbouj, M.; Inman, D.J. A review of vibration-based damage detection in civil structures: From traditional methods to Machine Learning and Deep Learning applications. *Mech. Syst. Signal Process.* **2021**, *147*, 107077. [CrossRef]
2. Cha, Y.-J.; Kim, Y.; You, T. Advanced Sensing and Structural Health Monitoring. *J. Sens.* **2018**, *2018*, 7286069. [CrossRef]
3. Bies, D.A. *Engineering Noise Control*; CRC Press: New York, NY, USA, 2017.
4. Fan, W.; Qiao, P. Vibration-based Damage Identification Methods: A Review and Comparative Study. *Struct. Health Monit.* **2010**, *10*, 83–111. [CrossRef]
5. Brincker, R.; Zhang, L. Frequency domain decomposition revisited. In Proceedings of the IOMAC 2009—3rd International Operational Modal Analysis Conference, Portonovo, Italy, 4–6 May 2009; pp. 615–626.

6. Amador, S.; Lysgaard, P.; Amador, S.D.R.; Brincker, R. Vibration-Based Damage Detection Using Input-Output and Output-Only Environmental Models: A Comparison. Available online: https://www.researchgate.net/publication/339310311 (accessed on 12 December 2021).
7. Sentosa, B.-O.-B.; Bui, Q.-B.; Ple, O.; Plassiard, J.-P.; Perrotin, P. Assessing Damage to Beam–Column Connections in Reinforced Concrete Structures from Vibrational Measurement Results. *Struct. Eng. Int.* **2019**, *29*, 396–403. [CrossRef]
8. Xu, G.Y.; Zhu, W.D.; Emory, B.H. Experimental and numerical investigation of structural damage detection using changes in natural frequencies. *J. Vib. Acoust. Trans. ASME* **2007**, *129*, 686–700. [CrossRef]
9. Ruggieri, S.; Fiore, A.; Uva, G. A New Approach to Predict the Fundamental Period of Vibration for Newly-designed Reinforced Concrete Buildings. *J. Earthq. Eng.* **2021**, 1–26. [CrossRef]
10. NEHRP Consultants Joint Venture. Soil-Structure Interaction for Building Structures. *Nist Gcr* **2012**, *12*, 917–921.
11. Gravett, D.Z.; Mourlas, C.; Taljaard, V.-L.; Bakas, N.; Markou, G.; Papadrakakis, M. New fundamental period formulae for soil-reinforced concrete structures interaction using machine learning algorithms and ANNs. *Soil Dyn. Earthq. Eng.* **2021**, *144*, 106656. [CrossRef]
12. Kabtamu, H.G.; Peng, G.; Chen, D. Dynamic Analysis of Soil Structure Interaction Effect on Multi Story RC Frame. *Open J. Civ. Eng.* **2018**, *08*, 426–446. [CrossRef]
13. Ratnika, L.; Gaile, L.; Vatin, N. Impact of Groundwater Level Change on Natural Frequencies of RC Buildings. *Buildings* **2021**, *11*, 265. [CrossRef]
14. Chopra, A.K.; Yim, S.C. Simplified Earthquake Analysis of Structures with Foundation Uplift. *J. Struct. Eng.* **1985**, *111*, 906–930. [CrossRef]
15. Trifunac, M.D.; Todorovska, M.I.; Manić, M.I.; Bulajić, B.Đ. Threshold changes in building frequencies of vibration associated with structural damage–study of full-scale observations in the Borik-2 Building in Former Yugoslavia. In Proceedings of the 14th World Conference on Earthquake Engineering, Beijing, China, 12–17 October 2008.
16. Hans, S.; Boutin, C. Dynamics of discrete framed structures: A unified homogenized description. *J. Mech. Mater. Struct.* **2008**, *3*, 1709–1739. [CrossRef]
17. Acikgoz, S.; DeJong, M.J. Analytical modelling of multi-mass flexible rocking structures. *Earthq. Eng. Struct. Dyn.* **2016**, *45*, 2103–2122. [CrossRef]
18. Ivanović, S.; Trifunac, M.; Novikova, E.; Gladkov, A.; Todorovska, M. Ambient vibration tests of a seven-story reinforced concrete building in Van Nuys, California, damaged by the 1994 Northridge earthquake. *Soil Dyn. Earthq. Eng.* **2000**, *19*, 391–411. [CrossRef]
19. Gallipoli, M.R.; Mucciarelli, M.; Šket-Motnikar, B.; Zupančić, P.; Gosar, A.; Prevolnik, S.; Herak, M.; Stipčević, J.; Herak, D.; Milutinović, Z.; et al. Empirical estimates of dynamic parameters on a large set of European buildings. *Bull. Earthq. Eng.* **2009**, *8*, 593–607. [CrossRef]
20. Oliveira, C.S.; Navarro, M. Fundamental periods of vibration of RC buildings in Portugal from in-situ experimental and numerical techniques. *Bull. Earthq. Eng.* **2010**, *8*, 609–642. [CrossRef]
21. Goel, R.K.; Chopra, A.K. Period Formulas for Moment-Resisting Frame Buildings. *J. Struct. Eng.* **1997**, *123*, 1454–1461. [CrossRef]
22. Gaile, L.; Sliseris, J.; Ratnika, L. Towards SHM of medium-rise buildings in non-seismic areas. In Proceedings of the 10th International Conference on Structural Health Monitoring of Untelligent Infrastructure, SHMII 10, Porto, Portugal, 30 June–2 July 2021; pp. 1–8.
23. Psycharis, I.N. Dynamics of flexible systems with partial lift-off. *Earthq. Eng. Struct. Dyn.* **1983**, *11*, 501–521. [CrossRef]
24. Palmeri, A.; Makris, N. Response analysis of rigid structures rocking on viscoelastic foundation. *Earthq. Eng. Struct. Dyn.* **2008**, *37*, 1039–1063. [CrossRef]
25. Di Trapani, F.; Bertagnoli, G.; Ferrotto, M.F.; Gino, D. Empirical Equations for the Direct Definition of Stress–Strain Laws for Fiber-Section-Based Macromodeling of Infilled Frames. *J. Eng. Mech.* **2018**, *144*, 04018101. [CrossRef]
26. Bathe, K.J. *Finite Element Procedures*; Englewood Cliffs: Prentice Hall, NJ, USA, 1996; p. 1037.
27. Knappett, J.; Craig, R.F. *Craig's Soil Mechanics*; CRC Press: London, UK, 2019. [CrossRef]
28. Akehashi, H.; Kojima, K.; Fujita, K.; Takewaki, I. Critical Response of Nonlinear Base-Isolated Building Considering Soil-Structure Interaction Under Double Impulse as Substitute for Near-Fault Ground Motion. *Front. Built Environ.* **2018**, *4*, 34. [CrossRef]
29. Gueguen, P.; Bard, P.Y. Soil-structure and soil-structure-soil interaction: Experimental evidence at the Volvi test site. *J. Earthq. Eng.* **2005**, *9*, 657–693. [CrossRef]
30. Hashemi, B.H.; Legzian, G.; Hosseini, M. A study on the behavior of structures based on the rocking motion of rigid cores involving pre-compressed springs and viscous dampers. *J. Vibroeng.* **2019**, *21*, 2180–2195. [CrossRef]
31. Nozari, A.; Behmanesh, I.; Yousefianmoghadam, S.; Moaveni, B.; Stavridis, A. Effects of variability in ambient vibration data on model updating and damage identification of a 10-story building. *Eng. Struct.* **2017**, *151*, 540–553. [CrossRef]